Active Optics Performance Study of the Primary Mirror of the Gemini Telescopes Project

Myung K. Cho

Optical Sciences Center in the University of Arizona
Tucson, AZ 85721
and
Gemini Telescopes Project
P. O. Box 26732
Tucson, AZ 85726-6732

Gemini Preprint #9

Active optics performance study of the primary mirror of the GEMINI Telescopes Project

Myung K. Cho

Optical Sciences Center in the University of Arizona
Tucson, AZ 85721
and
Gemini Telescopes Project
P. O. Box 26732
Tucson, AZ 85726-6732

ABSTRACT

A study on the evaluations of the active optics system performance for the primary mirror of the GEMINI Telescopes Project was conducted. Finite element analysis was employed to analyze the optical surface figures of the primary mirror. Four distinct influence matrices (generic 3-point kinematic system, combined unit case, 3-zonal multiple constraint system, and high frequency localized force set) were established based on the unit load cases at each of 120 active support locations and the restraint boundary conditions in the mirror model. A least square algorithm was developed. This scheme is able to accommodate the design constraints in the active optics systems. The active optics performances were evaluated by analyzing their capabilities in compensating the optical surface figures. For each active system, the level of the calculated active forces and the surface residual errors were examined. The results indicated that their performances are excellent and are in good agreement for most sampling surface figures. The results from the active optics performances based on the generic, the combined, and the 3-zone cases were practically identical for all the object surfaces. The active optics system based on the high frequency localized force set tends to predict a higher surface RMS error and requires a bigger force set. This effect became apparent when this system was applied to correct the surfaces from the natural mode analyses.

1. INTRODUCTION

Most large sized telescopes recently developed adopt a control system to actively correct the optical surface figure errors. Actively controlled optics system (active optics system) is applied to improve the optical surface quality to high precision optical systems subjected to selfweight loadings, external forces, thermal loadings, wind loadings, and other mechanical loadings. In common active optics system, for a given surface figure (object surface) a set of active forces at the actuator support locations is applied to the back of the primary mirror so that the object surface figure can be compensated. For a perfect active correction, the active optics force set will bring the surface back to the reference (undeformed) shape. Hence, the active forces must be carefully determined in order to increase the ability in correcting the object surface figure.

The surface quality in active optics system is mainly dependent upon the active loadings and the boundary restraint conditions. The following factors must be taken into account in calculation: the total number of the active supports, the support arrangement pattern and the support locations, the level of active force set, the defining support system, the stiffness of the mirror, and characteristics in the influence matrix. In general, the object surface figures in active system are predefined and are stored in a look-up table or an equivalent manner on a close loop. Those surfaces are quantified by means of experiments, mathematical expressions, or numerical approaches. An interferometric data set from a CCD array is used to quantify the optical surface figure in a test facility. For a low order frequency optical surface, it can be described as functions of mathematical expansions. Since the primary mirror substrate of large telescope is relatively flexible, its inherent flexibility to bending stiffness helps the optical surface to deform into desirable shapes with a moderate active force magnitude. The Zernike polynomials are commonly employed to describe these low order optical surface figures. For a numerical approach the Finite Element Method can be utilized. The surface figures are calculated based on imposed loading and boundary conditions. The resulting surface figures inherently include the effects from the restraints. Influence matrix, a set of surface deformations from the integrity of unit cases at each active support, can be established by a finite element analysis. Since the influence matrix is dependent upon the loadings and the boundary restraints, a choice of influence matrix may be trivial. Selection of the Influence matrix affects the optical performance of the active optics system.

The objective of this study is to demonstrate the performance of the active optics system applied to the primary mirror of the Gemini Telescopes Project. Four different active optics systems (generic 3-point kinematic system, combined unit case, 3-zonal multiple constraint system, and high frequency localized force set) will be examined and their results are to be evaluated with respect to the optical surfaces of typical gravity induced figure errors, the surfaces in Zernike polynomials, and the surface figures from the natural frequency modes. Each of these four active systems utilizes its distinct influence matrix established from the different unit load cases and the boundary restraint conditions.

2. DESCRIPTION OF THE GEMINI ACTIVE OPTICS SYSTEM

The primary mirror of the GEMINI Telescopes Project is a monolithic meniscus made from Corning ULE titanium-doped fused silica, which has a diameter of 8.1 m, a thickness of 20 cm, and a paraxial radius of curvature of 28.8 m. The mirror weight is approximately 23 metric tons. Since this primary mirror is a thin meniscus one, its inherent flexibility to bending stiffness helps the optical surface to deform into desirable shapes with a moderate active force magnitude. Refer to reference 1 for the support system and its design concept (axial supports, lateral supports, and air pressure support system).

The active optics system of the GEMINI primary mirrors is utilized to compensate the optical surface distortions due to the thermal variations, steady state wind, and support cell expansion. The active optics system is also to be designed to correct potential errors such as axial support errors (errors in force magnitude, angle, and position), lateral support errors, and air pressure errors (errors in pressure magnitude and forces of the air sealing). Additionally, the active system is capable of correcting the gravity sag of the secondary mirror as well as responding to the mirror figure change from the Cassagrain mode to the Ritchey-Chretien mode.

A set of 120 axial active actuators is located normal to the back of the primary mirror surface. These active actuators are arranged in five circular ring and are divided into a 'three-zone' or a 'six-zone' support system (see Figure 1). The development of optimum location and arrangement of these active actuators is described in References 2 and 3. In the active optics system of the GEMINI primary mirror, the magnitude of the active actuator forces and the force distribution depend upon a function of the operation mode (3-zone or 6-zone) of the distributed defining system. The applied active forces required to correct a surface figure may produce the same order of surface accuracy; however, the pattern and the level of forces are different between the three-zone and the six-zone modes [1,4,5].

A least square process was developed and used intensively for the primary mirror of the GEMINI Project which is capable of accommodating the design constraints and requirements for a general environment. A mathematical expression of the active optics equation as [6]:

$$[A]\,\{X\} = \{B\} \qquad (1)$$

where [A] is an influence matrix which is a predefined, {X} is an unknown force vector, and {B} is a given displacement vector which is an object optical surface figure. This least square scheme yields a solution with imposed design constraints from the above equation .

3. PERFORMANCE OF ACTIVE OPTICS SYSTEMS

A finite element model of the primary mirror was developed to establish influence matrices. The model consists of 2304 shell elements and 2304 nodes using I-DEAS™ software. This finite element mirror model is shown in Figure 2. A total of 120 unit load cases at each actuator location was considered. The optical surface deformations from the unit load cases were manipulated and stored into an influence matrix The influence matrix is used to evaluate the effect of a change in force at each of the 120 axial defining points, or a change in support point location, or both, on the primary mirror surface figure. For the surface quality evaluation, a least squares scheme was employed to determine the active force set and the surface residual error with the following constraints:

(1) The summation of forces on the mirror provided by the 120 axial defining points equals zero.
(2) The summation of moments about the center of the mirror equals zero.
(3) The maximum force of each axial support is not greater than 400 N.
(4) The optical surface deformation is minimized.
(5) Aberrations of piston, tilts, and focus were removed from the object surface figure in the least square process.

The evaluation of the active optics performances was studied based on the ability to compensate the optical surface figure errors and the maximum level of active force required. Four different influence matrices were established and their corresponding active systems are as follows:

(1) generic boundary restraints with a 'three kinematic mount'
(2) combined force system which redistributes reaction forces at the defining points
(3) three-zone multiple constraint system (three-zonal MPC case)
(4) localized high frequency force set in static equilibrium

Several sample optical surface figures were examined to evaluate the performance of these active optics systems with the design constraints in the least square process. Two typical selfweight induced surfaces were considered as examples of the gravity effects on the optical surface figure. Typical 36 Zernike surfaces described in FRINGE/PCFRINGE [7] was employed. Since the surfaces associated with rigid body motions (piston, tip, and tilt) and focus term were excluded, a total of 33 optical surfaces defined by the Zernike polynomials were used during the evaluation. Additionally, the optical surfaces corresponding to the first 16 characteristic modes were examined. These modes were selected from the first 41 natural frequency modes by a frequency analysis using the finite element method. This performance study includes the active optics capability to compensate these modal surface figures.

3.1. Generic Boundary Restraint Case (GENERIC)

To faithfully simulate a distortion of the optical surface due to external loads, a finite element mirror model needs to have proper boundary conditions. Theoretically, the mirror model must be in structurally stable and restrained to prevent the rigid body motions. As a simple way to support a mirror, a 'kinematic 3-point mount system' is commonly employed. When the mirror is subjected to a set of static loads, its optical surface will deform depending on the loading and the boundary conditions. If an optical system is held by a kinematic support, the structure is statically determinant. This implies that the system is not over restrained by the boundary supports. Hence it is in a stress free state. This is a very important aspect because the structure will deform only from the applied loads and the boundary restraints without experiencing secondary effects.

When a unit load is applied at an active actuator location with a kinematic support system, the resulting optical surface figure will include the effects from both the defining supports and the applied load. In other words, the mirror was exerted by a combined load condition with the unit load and the boundary reaction forces. For a kinematic mount system, at least three nodal points are required to be restrained for a full mirror model. Figure 3 shows a simple kinematic mount system. At all the defining points the translations along the optical axis (the z-axis) were prevented. Translations at any two locations were restrained in one direction (the y-axis) and translation along the other direction (the x-axis) was fixed. This boundary arrangement maintains the model in a stress free state as well as it provides the system in static equilibrium.

An influence matrix was constructed based on a total of 120 unit load cases under this kinematic boundary condition. Each element of this matrix (GENERIC) has inherent boundary restraint effects. An optical surface contour plot of a unit load is shown in Figure 4 as an example of an intermediate result during the process. This plot represents a surface figure for a unit load applied at support location #16 after removing aberrations of piston, tilts, and focus .

As mentioned above, GENERIC has inherent boundary restraint effects. However, a set of active forces calculated from the least square scheme guarantees that the reaction forces at the defining points vanish. It is obvious that the resulting active force set is in static equilibrium due to the imposed constraints in the active system equation.

3.2. Combined unit force system (COMBINED)

An attempt was conducted to attain an optical surface figure due to a unit load solely at an active support location excluding the effect from the kinematic boundary condition. This implies that in the finite element model the calculated reaction forces at the boundary need to be redistributed accordingly. This concept was originally developed by the WIYN telescope staffs and it was applied to the active optics system of the WIYN telescope [8]. The active optics system performance of WIYN has been reported with a great success and is believed as a 'proven technology'.

In WIYN, the hydraulic cylinders of the active support system are interconnected together in three zonal groups; therefore, a support force variation at one location is reacted by forces at the other support locations. The changes in active forces are resulted from a change in hydraulic pressure in each zone due to an applied force. Hence, the force system must satisfy the static equilibrium equations as follows:

$$\begin{aligned} &\text{sum } fi + Fj = 0 \\ &\text{sum } Mxi + Fj\ xj = 0 \\ &\text{sum } Myi + Fj\ yj = 0 \end{aligned} \qquad (2)$$

where fi is a change in an actuator force at the ith actuator location, Mxi and Myi are moments about the x-axis and the y-axis, respectively. Fj denotes the unit load applied at the jth actuator location and xj and yj are the coordinates. The change in the ith actuator force denoted fi is then

$$fi = Pk\ Ai \qquad (3)$$

where Pk is the pressure change in the kth zone and Ai is the area of a hydraulic cylinder at the ith location. From the above equations, a set of actuator forces can be determined. As typical combined unit force set, a unit load (1000 Newtons) applied at support #16 are listed in Table 1. A unit load case in this combined system is analogous to a set of forces in which one unit force at a given actuator location dominates the forces at all the other support locations.

An influence matrix based on these combined unit load cases (COMBINED) was created. The reaction forces at the kinematic boundary condition were calculated and they were verified to be zero. An optical surface contour plot of a combined unit load is shown in Figure 5 as an example of an intermediate result. This plot is for a unit case of support location #16 after removing aberrations of piston, tilts, and focus .

The COMBINED system is free from the effect of the boundary conditions. Since each unit load has a fully populated force array contributed by the forces at every actuator location, the resulting optical surface distortion shows a global effect. For this active optics system may not require the imposed force equilibrium constraints in the least square scheme. Each set of unit forces is inherently in a self equilibrium state.

3.3. Multiple point constraints in three zones (3-ZONE MPC)

The GEMINI support system is designed to operate in different modes. In three-zone kinematic mode being used in the WIYN Telescope primary mirror support, each of the support zone will have a master cylinder which controls the fluid volume in that zone. Net changes in the volume in each zone must be zero during the operation.

Implementation of Multiple point constraints (MPC) is used in solving a system of equation with multiple dependent variables. Whereas a single point constraint (SPC) is used for a single prescribed variable in the solution. Since the active actuators are interconnected in each zone, the individual active force becomes dependent one from another in a zone. The following boundary restraint conditions were applied to describe the three-zone MPC system of the GEMINI primary mirror:

$$\text{sum } dij = 0, \qquad \text{for } j=1,2,3 \qquad (4)$$

where dij is a displacement along the optical axis at the ith actuator location in the j zone.

An influence matrix (3-ZONE MPC) was established based on a total of 120 unit cases with the MPC conditions. 3-ZONE MPC uses a characteristic of the fluid volume invariant. Therefore, this represents a displacement based system. On the other hand, COMBINED used the hydraulic pressure invariant and it is a force based system.

Table 1. Typical combined unit force set for support #16
(a unit force of 1000 N is applied at support #16)

1	-25.79	2	-25.79	3	-1.6	4	-1.6	5	-1.6	6	-1.6
7	-25.79	8	-25.79	9	-25.79	10	-1.6	11	-1.6	12	-1.6
13	-1.6	14	-1.6	15	-1.6	16	974.21	17	-25.79	18	-25.79
19	-25.79	20	-1.6	21	-1.6	22	-1.6	23	-1.6	24	-1.6
25	-1.6	26	-1.6	27	-1.6	28	-25.79	29	-25.79	30	-25.79
31	-25.79	32	-25.79	33	-1.6	34	-1.6	35	-1.6	36	-1.6
37	-1.6	38	-1.6	39	-1.6	40	-1.6	41	-1.6	42	-1.6
43	-25.79	44	-25.79	45	-25.79	46	-25.79	47	-25.79	48	-25.79
49	-1.6	50	-1.6	51	-1.6	52	-1.6	53	-1.6	54	-1.6
55	-1.6	56	-1.6	57	-1.6	58	-1.6	59	-1.6	60	-1.6
61	-25.79	62	-25.79	63	2.39	64	2.39	65	2.39	66	2.39
67	-25.79	68	-25.79	69	-25.79	70	2.39	71	2.39	72	2.39
73	2.39	74	2.39	75	2.39	76	-25.79	77	-25.79	78	-25.79
79	-25.79	80	2.39	81	2.39	82	2.39	83	2.39	84	2.39
85	2.39	86	2.39	87	2.39	88	-25.79	89	-25.79	90	-25.79
91	-25.79	92	-25.79	93	2.39	94	2.39	95	2.39	96	2.39
97	2.39	98	2.39	99	2.39	100	2.39	101	2.39	102	2.39
103	-25.79	104	-25.79	105	-25.79	106	-25.79	107	-25.79	108	-25.79
109	2.39	110	2.39	111	2.39	112	2.39	113	2.39	114	2.39
115	2.39	116	2.39	117	2.39	118	2.39	119	2.39	120	2.39

An optical surface contour plot of typical unit load case is shown in Figure 6 as an example of an intermediate result. This plot illustrates a unit case of support location #16 after removing aberrations of piston, tilts, and focus. Since this system was restrained by displacement constraints in each zone, the resulting optical surface distortion is quite alike as COMBINED. However, this active optics system requires the imposed force equilibrium constraints in the least square process.

3.4. Localized high frequency force system (HIGH FREQ)

When an optical system is exerted by an external load set, there exists a set of reaction forces at the defining points. By applying an adapted force set to the system in order to counteract the given load, the system retains a self equilibrium state. However, there are infinite number of adapted force sets which satisfy the static equilibrium in the structural system. A few of them may or may not be practical in fulfilling imposed design requirements.

A parametric study was made to obtain a feasible force set for each unit load case. The following assumptions and design restraints were applied in this parametric study:

(1) the active support system is divided into three zones,
(2) the single unit load case comprises a set of four support forces (one master force and three slave forces),
(3) the forces are applied at the actuator locations within a zone,
(4) the force system must be in static equilibrium,
(5) maximum force at any slave location is limited to 60% of the master's,
(6) the force distribution must be highly localized for a high frequency optical surface distortion.

As a typical localized force set, a unit load (1000 Newtons) case for support #16 is shown in Figure 7. The corresponding set of forces (master and slave forces) is listed in Table 2. Noted that the line of action of these forces is normal to the mid plane of the mirror.

Table 2. Force Magnitudes of the master and the slaves (unit load case corresponding to support #16)

	Master	Slave 1	Slave 2	Slave 3
Support ID	16	7	76	29
Normal force (Newtons)	1000.00	-269.09	-363.12	-368.18

An influence matrix based on these localized high frequency unit load cases (HIGH FREQ) was established. An optical surface contour plot of a unit load case is shown in Figure 8 as an example of an intermediate result. This plot is for a localized unit case of support location #16 after removing aberrations of piston, tilts, and focus . Since in HIGH FREQ the system influence matrix contains highly localized surface figures, the resulting optical surface from this active optics system will be relatively coarse. This is resulted from a linear combination of the highly distorted individual unit load cases.

For this active optics system may not require the imposed force equilibrium constraints in the least square fit. Each set of unit forces is inherently in a self equilibrium state.

4. RESULTS OF ACTIVE OPTICS PERFORMANCES

In order to evaluated the performance of the four different active optics systems, a number of sample optical surface figures were examined. The design constraints and requirements proposed by the GEMINI Telescopes Project were applied during the least square process.

As typical selfweight induced optical surface deformations, two extreme gravity orientations, a ZENITH pointing position and a HORIZON pointing position, were considered. The surfaces corresponding to these gravity cases were examined and the performances were evaluated. For ZENITH, optical surface calculations were made based on a combined load comprised with the selfweight and a100% air pressure to balance the gravity. The optical surface figure has an RMS surface error of 130 nm after piston, tilts, and focus terms removed. As shown in Figure 9, the surface figure experienced a global distortion due to the gravity sag and the figure represents high order spherical aberrations. For the HORIZON position, the mirror is subjected to a combined load comprised with the lateral gravity and a set of lateral forces at a total of 60 lateral supports. The lateral support forces were designed to counteract the gravity load so that the system maintains a static equilibrium. This surface figure due the combined load has a high irregularity around the outer rim of the mirror where the lateral supports are located. The combined surface figure is shown in Figure 10. An RMS surface error of 10 nm was calculated after piston, tilts, and focus removed.

The performance of the active optics systems was evaluated by analyzing their abilities to compensate these two gravity induced surface figures. The results were listed in Table 3.

Table 3. Active optics system performances for surface figures in ZENITH and HORIZON locations

	Object	GENERIC		COMBINED		3-MPC		HIGH FREQ	
	(RMS)	(RMS)	(Fmax)	(RMS)	(Fmax)	(RMS)	(Fmax)	(RMS)	(Fmax)
ZENITH	130 nm	2 nm	20 N	2 nm	20 N	2 nm	20N	14 nm	110 N
HORIZON	10 nm	5 nm	18 N	5 nm	18 N	5 nm	18N	5 nm	18 N

The results indicated that the performances are quite compatible to one from another with exception of the case that HIGH FREQ was applied to the ZENITH position. In this cases, surface correction ability is low even though the force level is high. For the other cases, the results are excellent and are in good agreement.

An exercise was made to evaluate the ability of the active optics force correction systems to compensate for the primary surface figure shapes corresponding to the Zernike terms. A total of 33 Zernike aberrations defined in FRINGE/PCFRINGE was employed. A surface figure corresponding to each of the Zernike terms of 1000 nm surface RMS amplitude was assumed for the surface figure of the primary mirror. A set of 120 active force forces was applied to compensate the Zernike surface figures. Table 4 lists the residual surface RMS errors, and the maximum active force magnitudes to each Zernike term.

A frequency analysis was made using the finite element method to obtain the natural frequency modes. The model was analyzed under free loading and free boundary conditions (free-free BC's). Natural modes associated with the rigid body modes (six degrees of freedom in total) and the duplicated mode shapes were removed. In this study, a total of 16 reduced characteristic natural modes were considered. The 16 characteristic mode shapes are illustrated in Figure 11. The natural frequencies and their mode shapes of the GEMINI primary mirror were very similar to those of the VLT primary mirror [9]. Each surface figure was again normalized to a baseline surface RMS of 1000 nm. A set of 120 active force forces was applied to compensate the natural surface figures. Table 5 lists the residual surface RMS errors and the maximum active force magnitudes to each natural mode.

5. SUMMARY AND CONCLUSIONS

A study to evaluate the active optics system performance for the GEMINI primary mirror was conducted. Four different active optics systems were generated and were applied to the least square algorithm developed in the GEMINI Telescopes Project. The performance of the active optics systems was evaluated by analyzing their abilities to compensate surface figure shapes corresponding to the gravity induced deformations, Zernike polynomial expressions, natural frequency modes. Through the performance analysis with these sampling surfaces for the GEMINI primary mirror, the following summary and conclusions were made:

(1) For all four active optics systems, overall performances are excellent for most surface figures.
(2) The surface residual errors and the maximum active forces are in good agreement for most cases.
(3) Active optics systems based on GENERIC, COMBINED, and 3-ZONE MPC demonstrated practically identical performances.
(4) The active optics system based on HIGH FREQ tends to predict a higher surface RMS residual error with a bigger correction forces. This effect became apparent when HIGH FREQ was applied to correct the surface figures from the natural characteristic modes.

Table 4. Active optics performance for the Zernike surfaces
(normalized RMS surface errors of 1000 nm was used for each object Zernike surface)

	GENERIC		COMBINED		3_ZONE MPC		HIGH FREQ	
Zernike ID	rms (nm)	Fmax (N)	rms (nm)	Fmax (N)	rms (nm)	Fmax (N)	rms (nm)	Fmax (N)
4	3.2	28.94	3.2	28.96	3.2	28.34	3.8	39.1
5	3.3	30.48	3.3	30.48	3.3	30.53	3.9	54.84
6	41.9	355.71	42	353.5	42	351.79	42.4	371.91
7	41.9	327.68	42	325.33	42	325.78	41.7	331.47
8	177.7	513.86	178.3	507.21	178.3	498.23	177.5	585.69
9	13.4	110.04	13.4	109.86	13.4	109.65	13.9	132.02
10	13.4	102.2	13.4	102.17	13.4	101.65	14.5	105.88
11	87.5	787.15	87.7	788.2	87.8	768.56	87.9	788.12
12	90.6	809.54	90.6	809.58	90.6	810.51	90.9	888.28
13	241.1	1,814.26	243.1	1,787	243.1	1,791.99	242.9	1,794.03
14	242	1,641.48	243.1	1,612.35	243.2	1,613.89	241.8	1,662.41
15	436.7	1,994.16	437.9	1,968.1	438	1,978.33	439.8	2,063.75
16	28.9	243.48	28.9	243.5	28.8	242.96	29.1	255.75
17	25.3	249.13	25.3	249.14	25.3	249.89	25.8	285.25
18	160	1,527.4	160.1	1,524.48	160.1	1,529.76	160	1,483.08
19	160.2	1,457.7	160.2	1,457.31	160.2	1,455.67	160.2	1,502
20	371.1	2,343.25	372.1	2,347.71	372.3	2,251.5	371.8	36
21	383	2,439.76	383	2,439.75	383	2,442.88	382.1	2,576.88
22	598.9	3,026.72	600.3	2,928.93	600.2	2,921.63	600.7	3,183.81
23	599.4	3,041.16	600.2	3,032.61	600.4	2,934.59	595.4	3,092.25
24	775.5	1,671.98	777.3	1,629.68	777.5	1,862.89	776.3	2,436
25	45.4	433.87	45.4	433.89	45.4	436.35	48.1	566.84
26	45.3	403.47	45.3	403.48	45.3	403.78	48.2	609.38
27	243.4	2,414.97	243.4	2,415.21	243.3	2,404.05	241.8	2,544.5
28	246.4	2,456.65	246.4	2,456.65	246.6	2,467.59	245.6	2,506
29	512.4	3,307.68	512.5	3,313.61	512.6	3,303.05	511.3	3,553.62
30	512.8	3,210.24	512.9	3,215.94	512.8	3,212.26	511	3,351.75
31	690.2	2,95355	691.3	2,635.01	691.5	2,631.16	689.9	3,040.75
32	716.8	2,868.05	716.8	2,867.48	716.9	2,837.63	715.2	2,992.38
33	752.7	3,121.24	757.9	1,609.88	758	1,633.15	757.8	2,068
34	755.2	1,578.63	758	1,589.75	758.1	1,535.21	753	2,626
35	708.2	2,320.97	709.1	2,404.09	709.1	2,408.55	708.4	2,597.9
36	909.8	1,292.44	932.1	1,296.33	932.2	1,206.15	923.6	1,918

Table 5. Active optics performance for 16 characteristic natural modes
(normalized RMS surface errors of 1000 nm was used for each object modal surface)

	GENERIC		COMBINED		3_ZONE MPC		HIGH FREQ	
Mode ID	rms (nm)	Fmax (N)	rms (nm)	Fmax (N)	rms (nm)	Fmax (N)	rms (nm)	Fmax (N)
1	0.1	5.07	0.1	5.07	0.1	5.09	2.5	46.47
2	70.4	312.64	70.5	315.65	70.6	322.76	71.6	424.23
3	0.5	29.45	0.5	29.45	0.4	28.99	5.6	102.85
4	1.4	74.23	1.5	81.01	1.3	75.01	8	468.94
5	1.2	90.01	1.2	90.01	1.2	90.22	6.4	134.98
6	2.9	223.33	2.9	223.33	2.8	224.34	21.9	508.4
7	3.8	169.24	3.8	169.25	3.8	168.71	11.8	328.37
8	5.2	208.53	5.2	207.57	5.3	214.88	10.5	340.09
9	5.9	449.35	5.9	449.36	5.9	448.58	35.5	758.15
10	9.4	367.25	9.4	367.21	9.5	363.7	24	599.53
11	13.2	548.99	13.3	547.37	13.4	543.7	24.4	647
12	10.7	818.2	10.7	818.21	10.7	816.76	35.8	955.5
13	19.2	731.99	19.2	731.99	19.2	733.1	31.8	1,086.5
14	29	931.38	29	931.43	29	930.66	37.9	1,455.41
15	18	1,311.57	18	1,311.56	17.8	1,307.08	68.4	2,095
16	47.2	967.45	48.3	966.68	48.2	961.54	49.2	1,043.5

(5) In HIGH FREQ, a choice of localized force set is trivial and the performance may vary with a difference force arrangement.

6. ACKNOWLEDGMENTS

The Gemini 8m Telescopes Project is managed by the Association of Universities for Research in Astronomy, for the National Science Foundation, under an international partnership agreement. The author would like to acknowledge the contributions made to this paper by Earl Pearson and Larry Stepp of the Gemini 8m Telescopes Project.

7. REFERENCES

1. L. M. Stepp, E. W. Huang, and M. K. Cho, "Gemini primary mirror support system," Advanced Technology Optical Telescopes V, SPIE Vol. 2199, March, 1994.

2. M. K. Cho and R. S. Price, "Optimization of support point locations and force levels of the primary mirror support system," GEMINI Telescopes Project, RPT-O-G0017, 1993.

3. M. K. Cho and R. S. Price, "Theoretical active optics performance of the Gemini 8-m primary mirror," GEMINI Telescopes Project, RPT-O-G0032, 1993.

4. E. Huang, "Response of the primary mirror to wind loads," GEMINI Telescopes Project, RPT-O-G0035, 1993.

5. L. M. Stepp and M. K. Cho, "The distributed defining system for the primary mirrors," GEMINI Telescopes Project, RPT-O-G0023, 1993.

6. M. K. Cho, "Optimization strategy of axial and lateral supports for large primary mirrors," Advanced Technology Optical Telescopes V, SPIE Vol. 2199, March, 1994.

7. M. K. Cho and R. M. Richard, "PCFRINGE - An optical performance program using structural deflections (version 3.2), the Optical Sciences Center at the University of Arizona, Tucson, Arizona, 1990.

8. L. M. Stepp, D. Dryden, R. Nicolas, and M. K. Cho, "Actively controlled 3.5-m WIYN Telescope," Active and Adaptive Optical Systems, SPIE Vol. 1542, July, 1991.

9. P. Dierickx, "Polynomial expression of the sixteen first natural modes of the VLT primary mirrors," ESO VLT, VLT-SPE-ESO-11110-0006, 1992.

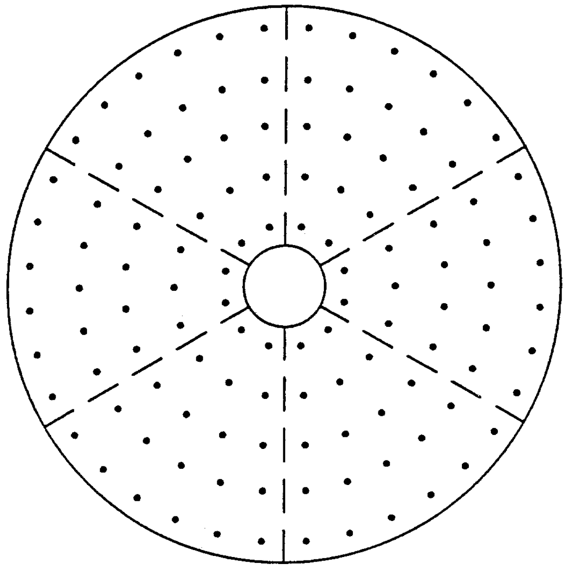

Figure 1. The location of the 120 active supports.

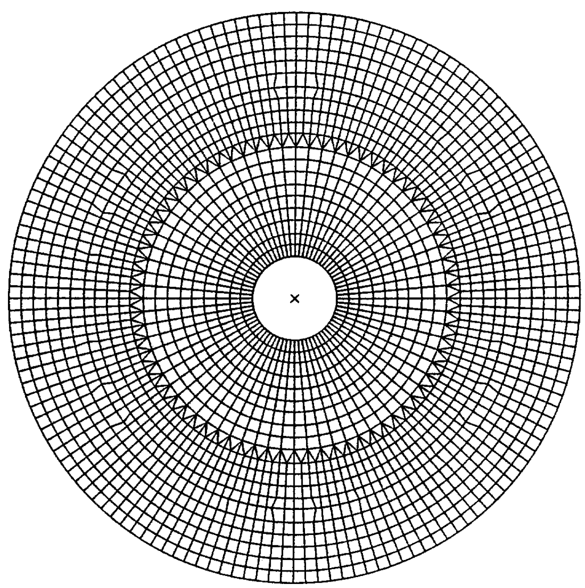

Figure 2. Finite element model used for the active optics performance analysis.

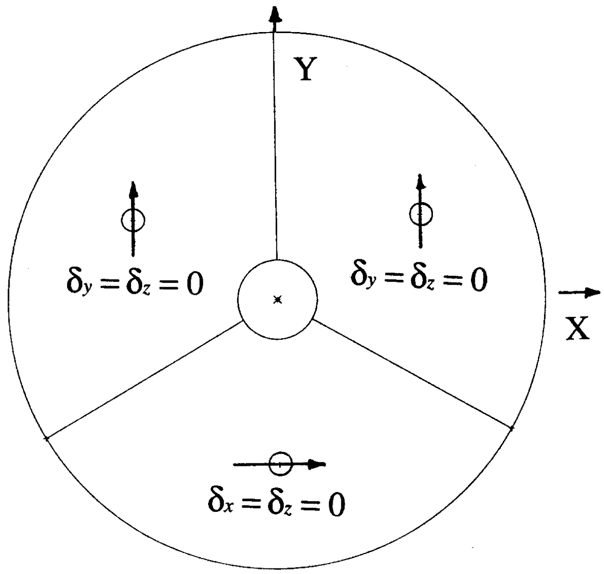

Figure 3. Typical three-point kinematic mounting system.

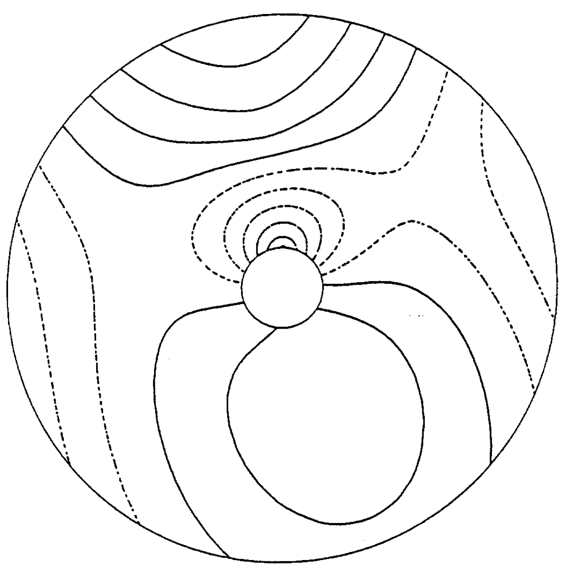

Figure 4. Unit load case of support #16 for the GENERIC active optics system.

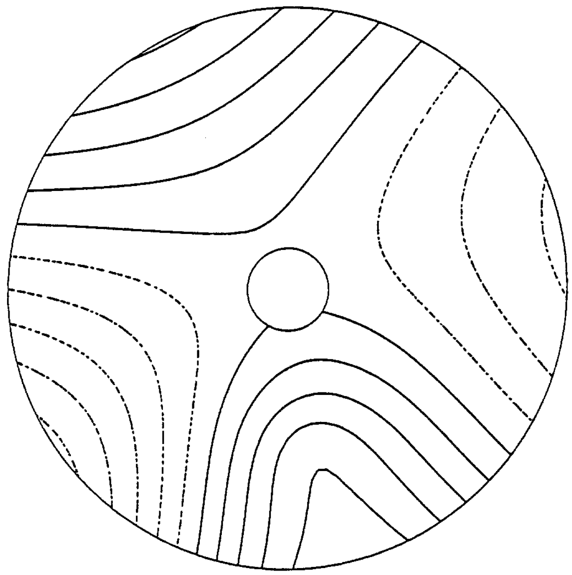

Figure 5. Unit load case of support #16 for the COMBINED active optics system.

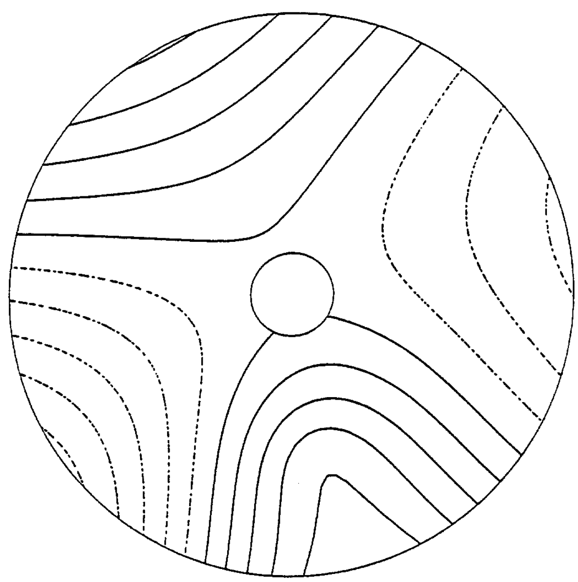

Figure 6. Unit load case of support #16 for the 3-ZONE MPC active optics system.

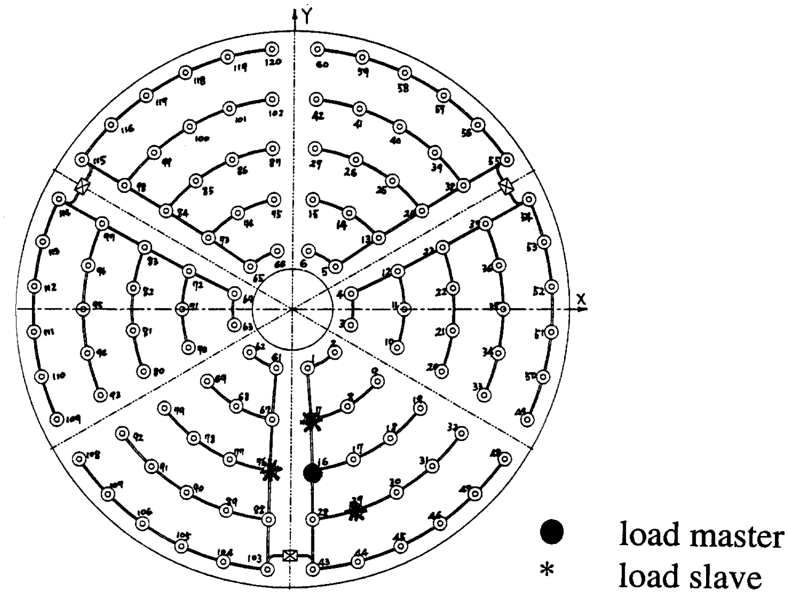

Figure 7. The localized force set of the unit load case of support #16.

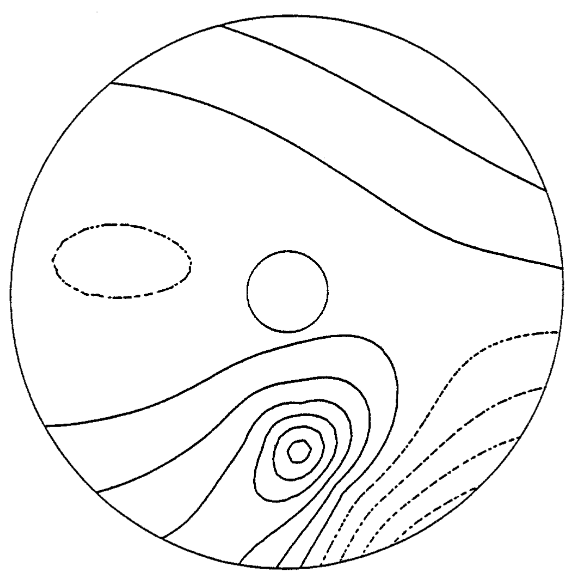

Figure 8. Unit load case of support #16 for the HIGH FREQ active optics system.

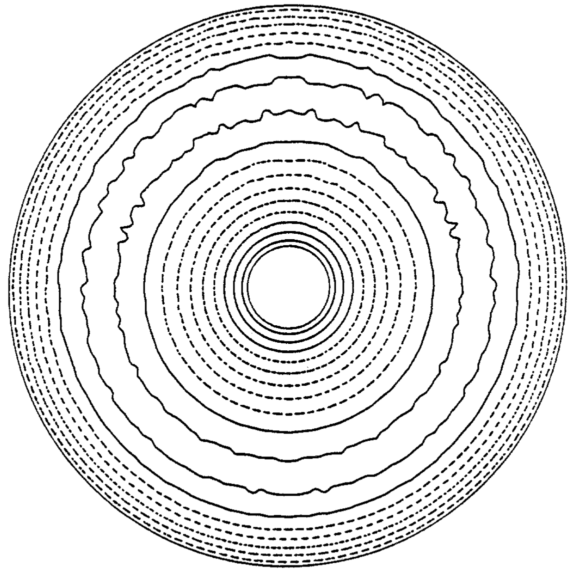

Figure 9. Optical surface map for the primary mirror in the ZENITH position.

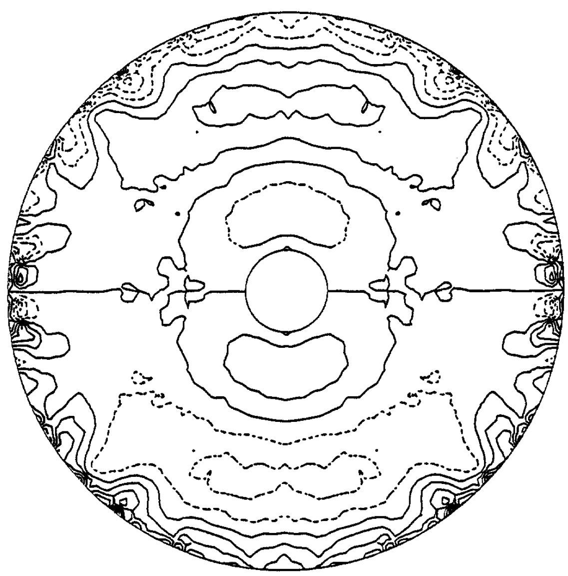

Figure 10. Optical surface map for the primary mirror in the HORIZON position.

Natural Frequencies of GEMINI Primary Mirrors

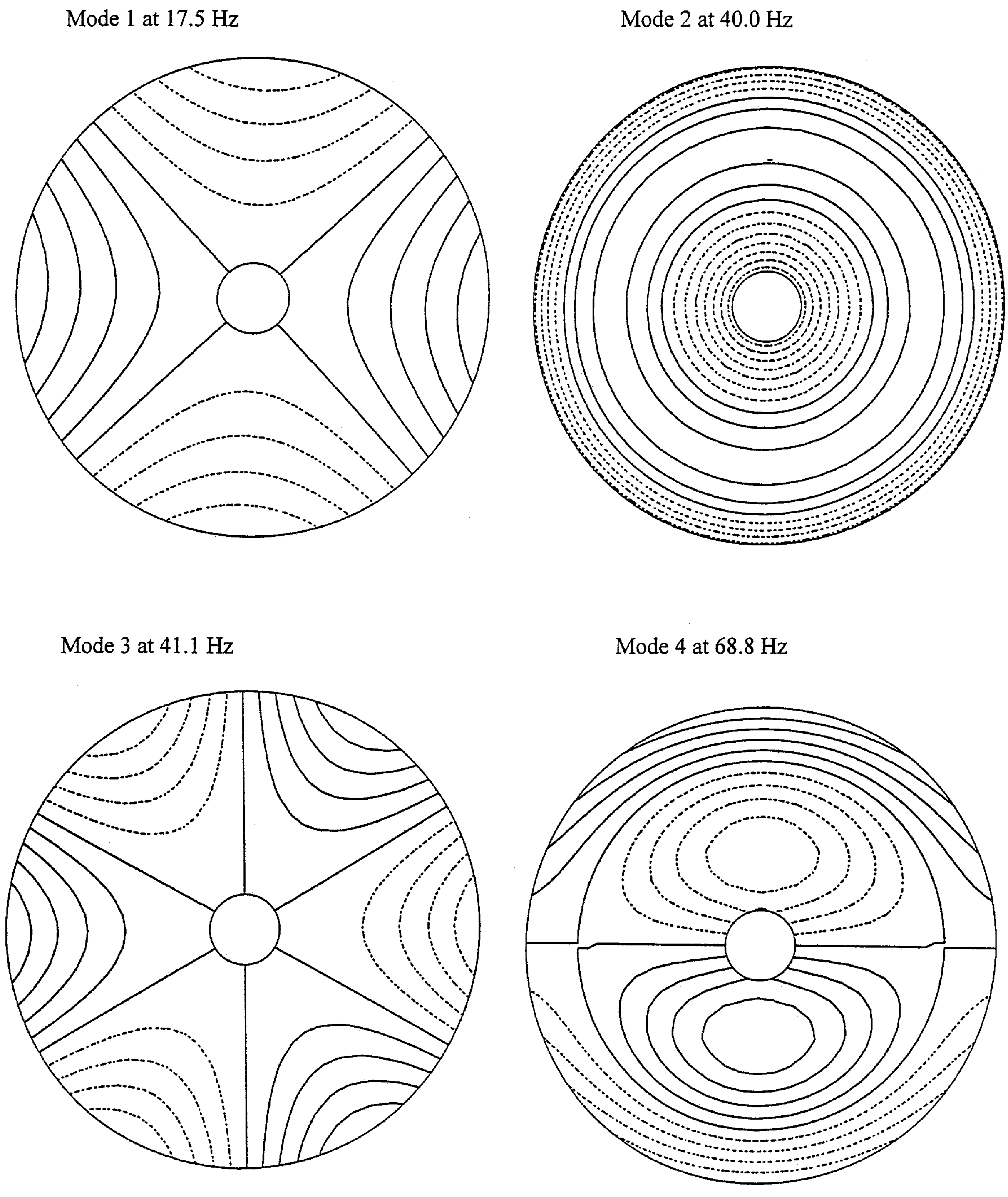

Figure 11. The first 16 natural modes of the GEMINI primary mirror.

Natural Frequencies of GEMINI Primary Mirrors

Mode 5 at 71.3 Hz

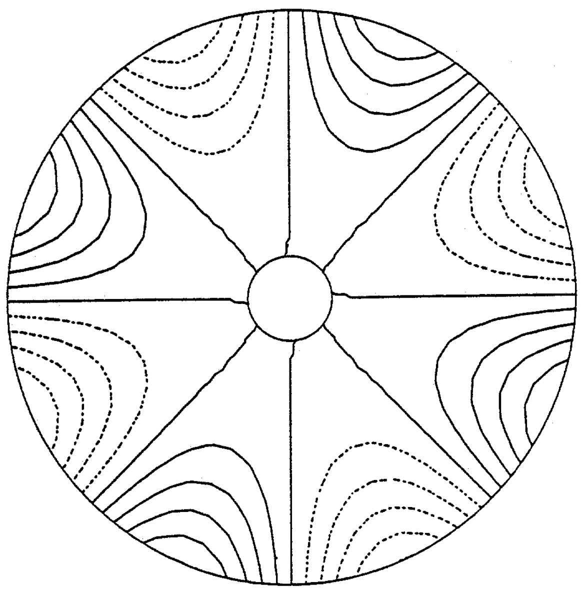

Mode 6 at 108.4 Hz

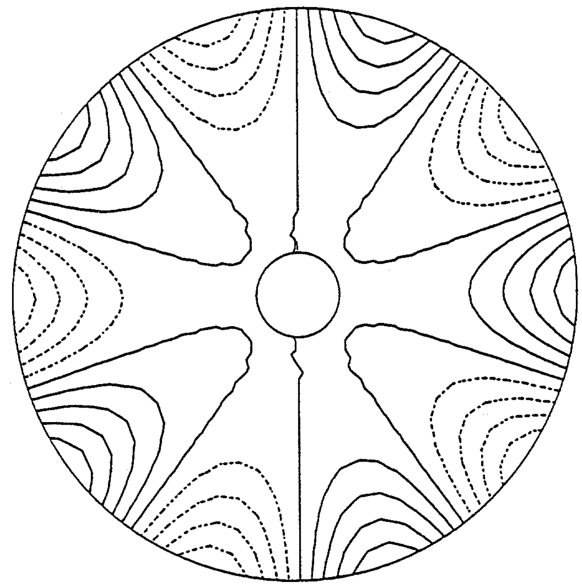

Mode 7 at 109.1 Hz

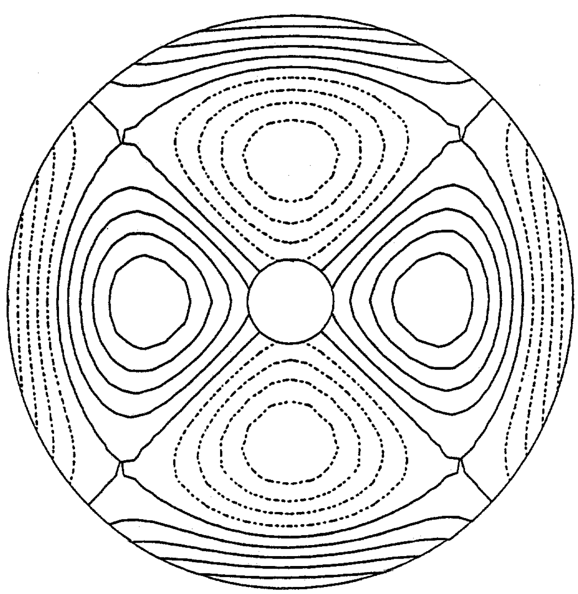

Mode 8 at 124.3 Hz

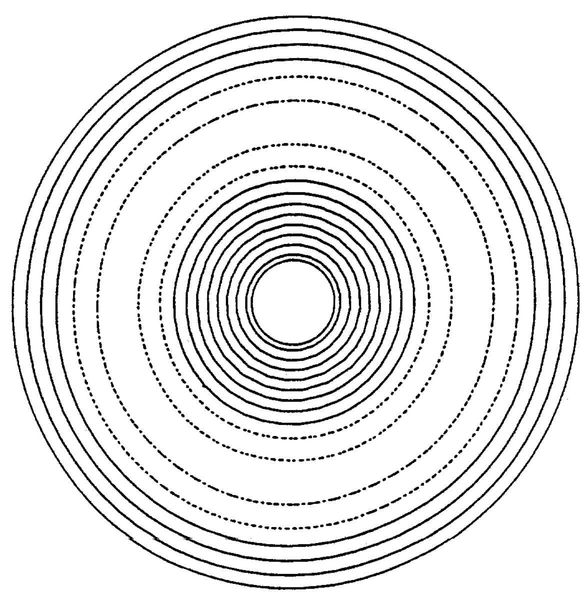

Figure 11. The first 16 natural modes of the GEMINI primary mirror - continued.

Natural Frequencies of GEMINI Primary Mirrors

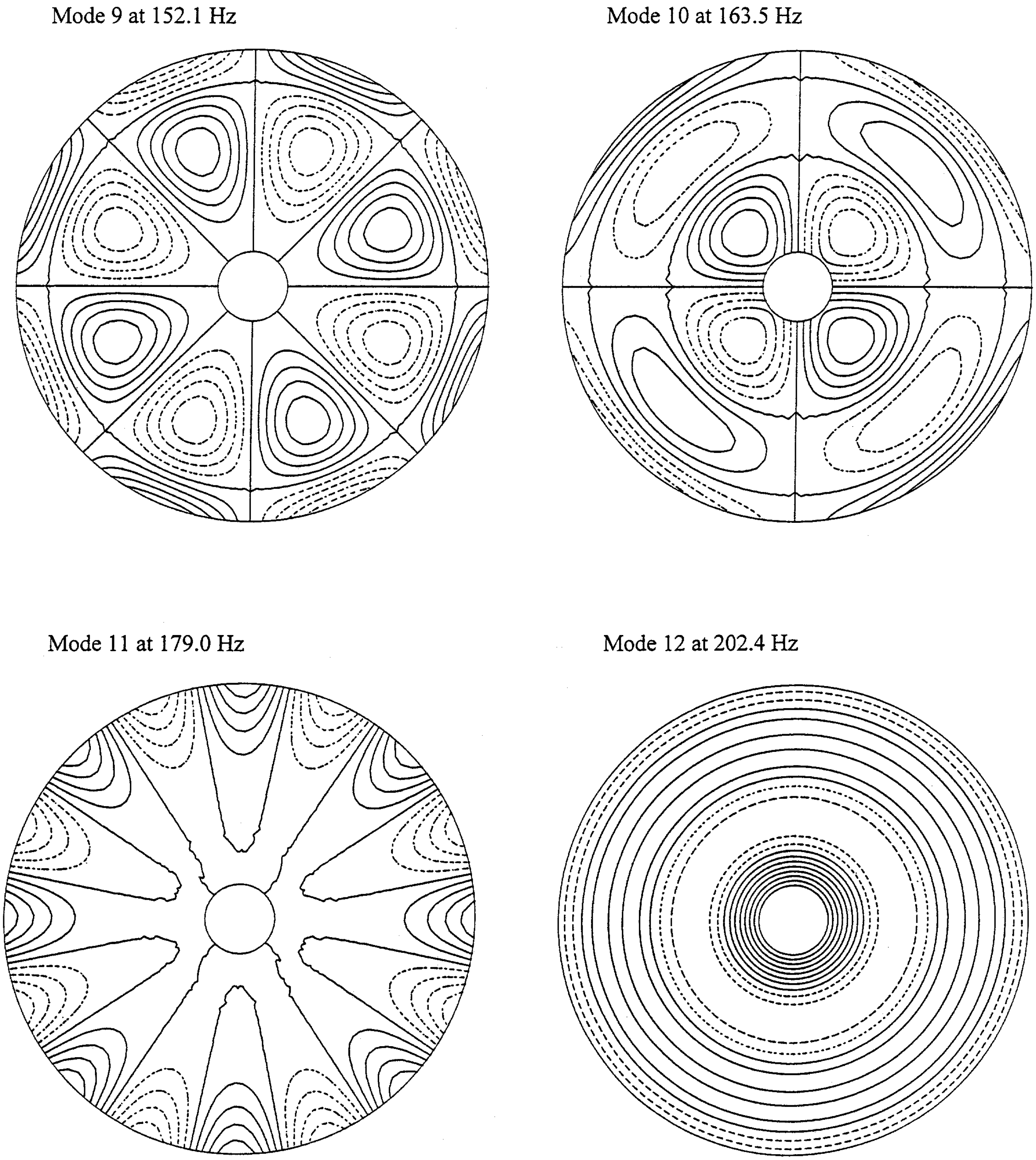

Figure 11. The first 16 natural modes of the GEMINI primary mirror.

Natural Frequencies of GEMINI Primary Mirrors

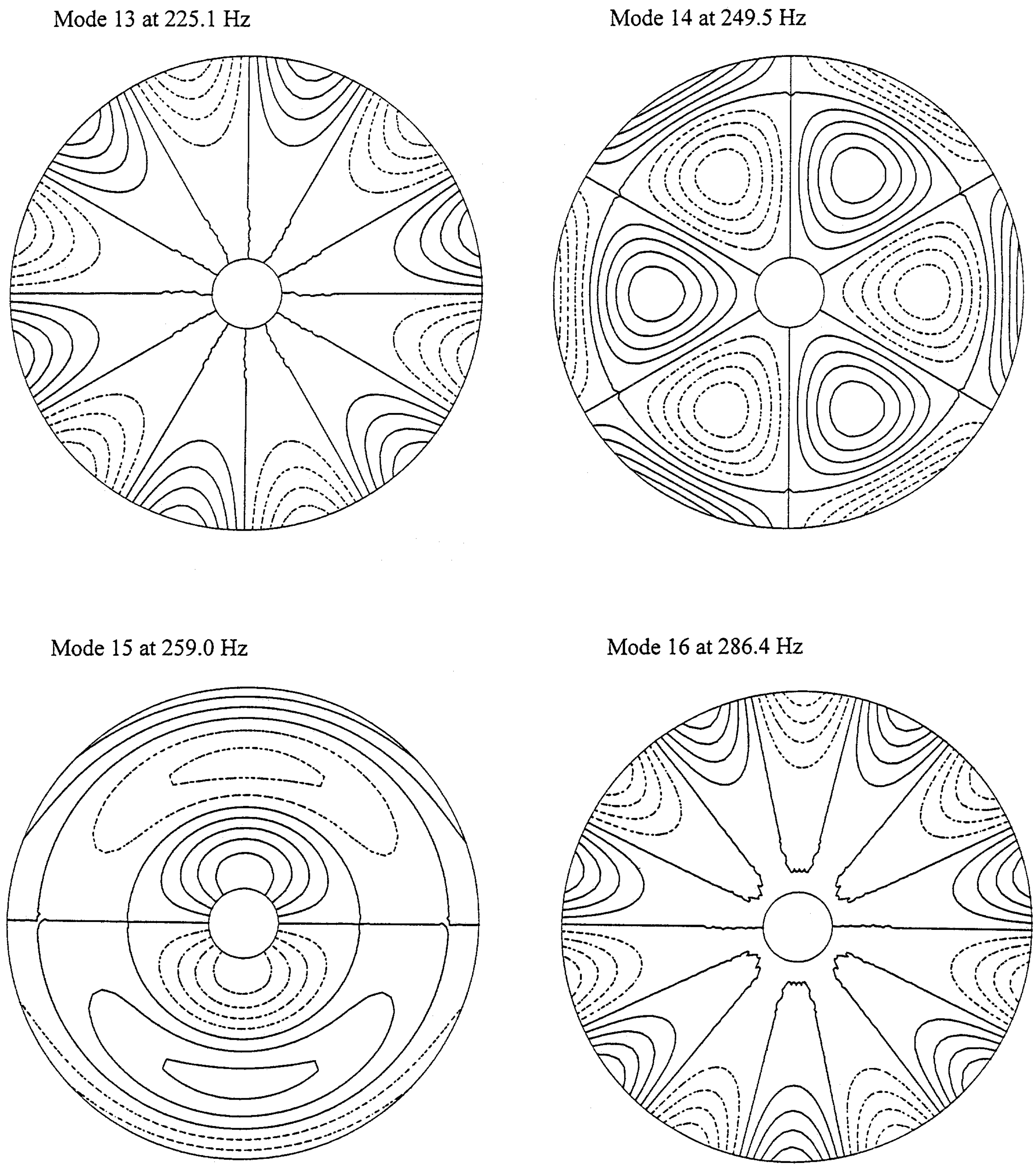

Figure 11. The first 16 natural modes of the GEMINI primary mirror.